Transportable Optical Lattice Clock with 7×10^{-17} Uncertainty

S. B. Koller, J. Grotti, St. Vogt, A. Al-Masoudi, S. Dörscher, S. Häfner, U. Sterr, and Ch. Lisdat
Physikalisch-Technische Bundesanstalt, Bundesallee 100, 38116 Braunschweig, Germany
(Received 20 September 2016; published 13 February 2017)

We present a transportable optical clock (TOC) with ^{87}Sr. Its complete characterization against a stationary lattice clock resulted in a systematic uncertainty of 7.4×10^{-17}, which is currently limited by the statistics of the determination of the residual lattice light shift, and an instability of $1.3 \times 10^{-15}/\sqrt{\tau}$ with an averaging time τ in seconds. Measurements confirm that the systematic uncertainty can be reduced to below the design goal of 1×10^{-17}. To our knowledge, these are the best uncertainties and instabilities reported for any transportable clock to date. For autonomous operation, the TOC has been installed in an air-conditioned car trailer. It is suitable for chronometric leveling with submeter resolution as well as for intercontinental cross-linking of optical clocks, which is essential for a redefinition of the International System of Units (SI) second. In addition, the TOC will be used for high precision experiments for fundamental science that are commonly tied to precise frequency measurements and its development is an important step to space-borne optical clocks.

DOI: 10.1103/PhysRevLett.118.073601

The best clocks reach fractional systematic uncertainties of a few 10^{-18} [1–3] and instabilities near or even below $10^{-16}/\sqrt{\tau}$ [1,4–6], surpassing the clocks realizing the International System of Units (SI) second in both aspects by 2 orders of magnitude. These achievements have triggered a discussion about a redefinition of the SI second [7,8] and push the frontiers of precision spectroscopy [2,9,10] as well as tests of fundamental physics [10–13]. Further, these clocks enable chronometric leveling [14–18] with relevant resolution, where gravitational redshifts are exploited to measure height differences.

So far, the operation of optical clocks has been constrained to laboratories. However, applications like chronometric leveling require transportable clocks to provide the necessary flexibility in the choice of measurement sites. Transportable optical clocks (TOCs) are highly interesting for frequency metrology and time keeping as well, enabling a consistent worldwide network of ultraprecise clocks. Although comparisons at the full performance level of state-of-the-art optical clocks are possible through a few specialized optical fiber links [19–22] on a continental scale [17,23], intercontinental links are restricted to satellite-based methods that do not reach the clock performance [24]. In contrast, a transfer standard enables world-wide interconnections between optical clocks exploiting their exquisitely small uncertainty and low instability. It will thus benefit the efforts towards a redefinition of the SI second.

Making optical clocks compact and robust for transport is the first phase in granting a wide community of users access to these devices [25–27]. Furthermore, transportability is a relevant step towards applications of optical clocks in space. Although developments in these directions are ongoing [28–31], to our knowledge, the only other transportable clock with an uncertainty below 10^{-16} is a single-ion clock reported recently [31].

The requirements on such a TOC are challenging indeed: To enable high-level comparisons of optical clocks it should achieve uncertainties similar to those of the clocks to be tested. In any case, significantly smaller uncertainties than in comparisons via primary cesium clocks [9,10,32,33] must be reached.

For geodetic applications, i.e., chronometric leveling, a resolution of below ten centimeters is required to compete with established methods that connect sites separated by several hundreds of kilometers. In other words, fractional gravitational redshifts of 10^{-17} and below must be resolved by the TOC. Additionally, the frequency instability should be in the range of $10^{-15}/\sqrt{\tau}$ or better to reach these uncertainties in considerably less than one week of accumulated measurement time.

These requirements are considerably beyond the properties achieved with the best transportable clocks [31,34]. For the atomic cesium fountain clock [34] an uncertainty of 5.9×10^{-16} [35] and an instability of $1.8 \times 10^{-13}/\sqrt{\tau}$ [36] have been reported. These properties were pivotal in several campaigns [25–27]. The $^{40}Ca^{+}$ ion clock reported in Ref. [31] reaches an uncertainty of 7.7×10^{-17} and an instability of $2.3 \times 10^{-14}/\sqrt{\tau}$, but has not left the laboratory yet. Here we present a transportable optical lattice clock (OLC) that is characterized and compared to an established, stationary optical frequency standard [5,9,17,33]. Then it has been installed in a car trailer (Fig. 1) and successfully applied in two off-campus measurement campaigns.

The clock uses the $(5s^2)^1S_0 - (5s5p)^3P_0$ transition in ^{87}Sr at 698 nm as reference transition, which is interrogated in atoms laser cooled into a one-dimensional optical lattice. The OLC comprises four main parts: The physics package, in which the atoms are prepared and the reference transition is interrogated; the laser systems for laser cooling, state

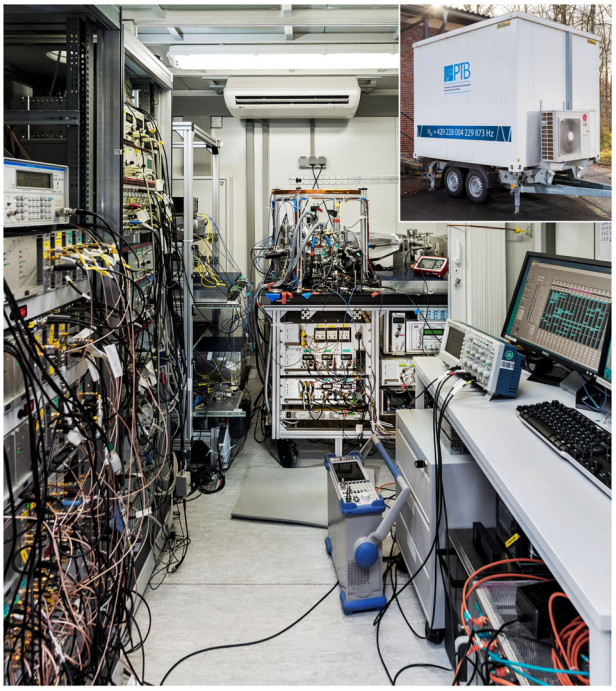

FIG. 1. View into the car trailer for transport and operation. Front, left: Electronics for the laser systems. Back, left: Laser systems for cooling and trapping, and the reference cavities to frequency stabilize these lasers. Back center: Physics package. Front right: Computer control. Not shown are the interrogation and lattice laser setups. The interior dimensions of the container are 2.2 m × 3 m × 2.2 m. The mass of the depicted experimental setup is approximately 800 kg. Inset: The car trailer from outside.

preparation, and trapping; a highly frequency-stable interrogation laser system; and the computer control to generate the experimental sequence and feedback to the interrogation laser frequency. For a TOC it is essential that these parts are compact in size and robust in construction to provide fast and reliable measurements at different locations.

Our cooling and preparation laser systems use commercial diode lasers integrated into five compact modules with half-inch optics [37,38]. These contain acousto-optical modulators (AOMs) and optical shutters for frequency modulation and light switching. They are connected to the physics package by polarization maintaining fibers. The modules have a size of 30 cm × 45 cm × 6 cm and a mass of less than 8 kg each. Since we do not aim for extreme compactness, we use standard control electronics.

Similarly, the compact physics package is mounted on a 120 cm × 90 cm optical breadboard. It has not been miniaturized to avoid trade-offs with the clock performance. The Zeeman slower, for efficiently loading atoms into a magneto-optical trap (MOT), is based on permanent magnets to avoid heat load from a solenoid near the interrogation region of the atoms [38]. Given the small volume available for a transportable setup, this helps in preventing thermal inhomogeneities of the physics package and thus of the environment of the atoms. This is important, since the blackbody radiation (BBR) shift is typically the largest source of uncertainty in Sr OLCs that are operated in room-temperature environments [1,39,40]. The physics package and laser systems have been tested successfully in the car trailer, achieving similar atom numbers and temperatures as in the laboratory. The height difference of the atoms respective to an outside reference on the car trailer is fixed within a few millimeters by the geometry of the physics package.

The reference cavity to prestabilize the frequency of the interrogation laser is a highly critical part of the TOC. An assembly with standard soft supports (e.g., Ref. [44]) would not withstand transport. Therefore, rigid mounting [45,46] is employed in our reference cavity as shown in Fig. 2. This laser system is a further development of an earlier cavity-stabilized laser system [47] and reaches a frequency instability flicker floor of about 4×10^{-16} after 10 s. For best performance in a measurement, the 12 cm long reference cavity and the interrogation laser are placed outside the car trailer in a seismically quieter environment.

The measurement sequence is comparable to other ^{87}Sr OLCs. Typically, the cycle time is 900 ms with a duty factor of 0.16: Atoms from a 480 °C hot oven are loaded via the Zeeman slower for about 300 ms into the magneto-optical trap (MOT). This MOT loading stage on the 461 nm $^1S_0 - {}^1P_1$ transition is followed by a second cooling stage using the 689 nm $^1S_0 - {}^3P_1$ transition, which is split into a broadband red MOT (80 ms) and a single-frequency MOT (80 ms), during which the optical lattice is loaded. The lattice is tilted by approximately 50° against gravity and operated at the Stark shift cancellation wavelength near 813 nm [48]. The full trap depth is typically about 80 E_r, where E_r is the lattice

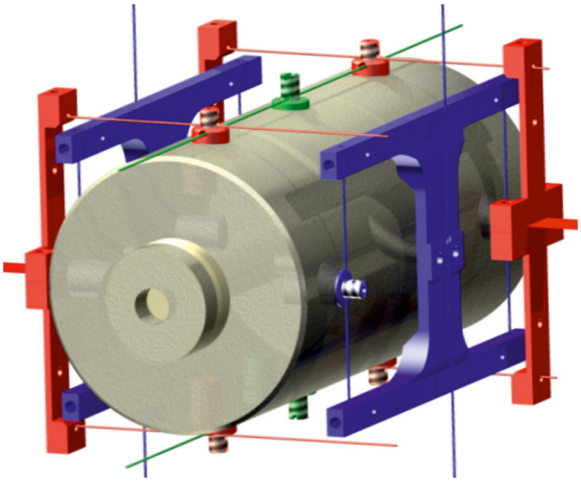

FIG. 2. Sketch of the transportable reference cavity of the interrogation laser. The cavity is fixed to wires at ten points as indicated in red, green, and blue. These mounting points lie in the corresponding symmetry planes of the cavity to minimize vibration sensitivities. The wires are held by flexibly mounted bars to avoid stress on the cavity by mechanically overdetermined mounting. Each color-coded set of mounting elements restricts 1 rotational and 1 translational degree of freedom.

photon recoil energy. The atoms trapped in the lattice are spin-polarized alternatingly to one of the stretched state ($|m_F| = 9/2$) of the ground state manifold (30 ms). To remove the atoms in other Zeeman levels (clean-up), a π pulse drives the atoms from the chosen Zeeman state on a resonant π transition in a magnetic field of about 1.9 mT to the $^3P_0$ state (30 ms). Atoms remaining in the $^1S_0$ manifold are expelled from the lattice by a pulse of 461 nm light (10 ms). The actual interrogation is performed in a magnetic field of about 45 μT parallel to the linear polarization of the lattice with a Rabi π-pulse duration in the range of 100 ms to 150 ms producing Fourier-limited spectra. A rotary atom shutter is used to shield the atoms from the BBR of the oven during the interrogation. Opening or closing the shutter takes 10 ms. We wait for an additional 90 ms after opening, which increases the stability of the atom number in the lattice. We use a normalized electron-shelving detection technique [49] by applying a combination of the 461 nm fluorescence detection with 707 nm and 679 nm light to repump the atoms to the ground state in order to determine the excitation probability at the frequency of the interrogation laser.

We apply this technique on both half-width points of each $\pm 9/2$ transition. A computer program evaluates these four interrogations and tracks the center frequency, the linear Zeeman splitting, and drift of the reference cavity. In this way, it stabilizes the interrogation laser to the linear-Zeeman-shift-free transition frequency.

To evaluate the TOC, we perform a direct comparison with our stationary ^{87}Sr OLC at Physikalisch-Technische Bundesanstalt [5,9,33]. The beat frequency between the two interrogation lasers is recorded with a dead-time-free counter. No elements of the two clocks are shared such that the two clocks are fully independent. The instability of their frequency ratio $\nu_{\mathrm{trans}}/\nu_{\mathrm{stat}}$, as expressed by the total Allan deviation, is about $1.3 \times 10^{-15}/\sqrt{\tau}$ as shown in Fig. 3. It is governed by the transportable clock, since the stationary system exhibits an instability in the low $10^{-16}/\sqrt{\tau}$ range [5]. The instability of the TOC is dominated by the performance of the interrogation laser [45] through the Dick effect [50]. It is lower than achieved in typical single ion clocks [3,12,31,51], and comparable to many high performance lattice clocks [2,32,52–56].

Beyond the instability of the transportable clock, the ratio measurements also test the agreement of both Sr OLCs within their uncertainties. The uncertainty of the stationary clock has been evaluated repeatedly and its frequency compared with primary Cs clocks [9,33,49] and another Sr OLC down to a fractional uncertainty of 5×10^{-17} [17].

The uncertainty of the TOC was evaluated along the same lines as discussed for our stationary system [33,49]: The BBR shift causes the largest fractional correction of about 5×10^{-15}. To ensure a precise control of this shift, even in a less temperature-stable environment than a laboratory, constructional details of the physics package

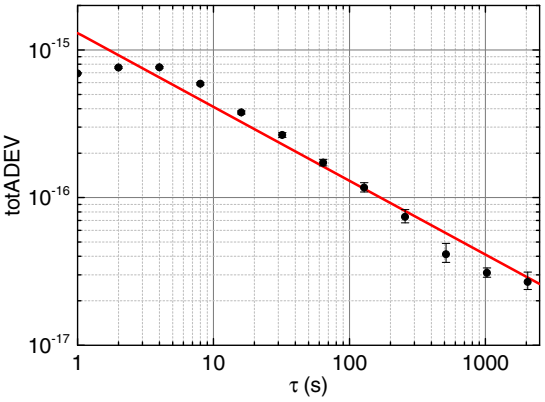

FIG. 3. Total Allan deviation (totADEV) of the frequency ratio $\nu_{\mathrm{trans}}/\nu_{\mathrm{stat}}$ (dots). The solid line indicates an instability of $1.3 \times 10^{-15}/\sqrt{\tau}$.

are important. We avoid excessive power dissipation in the physics package by using the Zeeman slower mentioned above. For generating the MOT and bias magnetic fields, we opted for compact coils with efficient water cooling through hollow wires as shown in Fig. 4. Note that the windings adjacent to the vacuum chamber are closest to the coolant inlet and are effectively isolating the windings with the warmed-up coolant from the vacuum chamber. The cooling water temperature is stabilized to better than 100 mK by a thermostat, which not only removes the energy dissipated in the coils, but effectively stabilizes the temperature of a large part of the environment of the atoms. By adjusting the temperature of the coolant, we minimize the temperature difference of the warmest (T_{max}) and coolest (T_{min}) spots of the vacuum chamber. The temperature is measured at eight locations outside and inside the

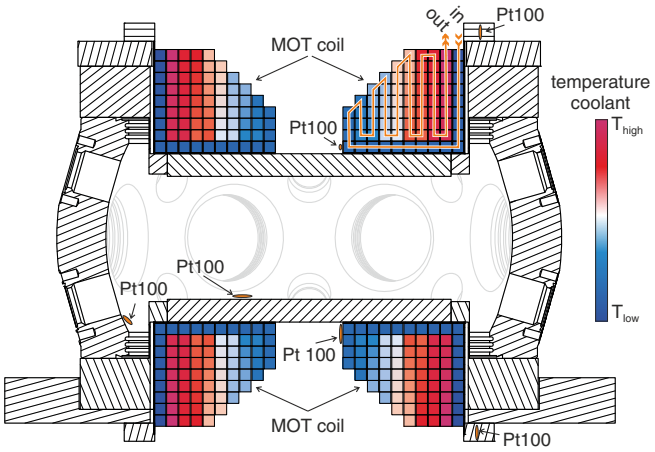

FIG. 4. Section through the main vacuum chamber. The MOT coils wound from hollow, square wires with the coolant in the bore are located in reentrant flanges. The layout is indicated by the coolant flow and the color-coded coolant temperature. The windings exposed to the chamber are cooled first and are thus temperature-controlled best. The locations of some Pt100 temperature sensors are also indicated.

TABLE I. Corrections (corr.) and uncertainties (unc.) of the transportable and stationary clock in parts per 10^{17}.

Effect	Transportable		Stationary	
	corrections	uncertainties	corrections	uncertainties
BBR ac Stark shift	488.3	0.9	492.4	2.3
BBR oven	0	0	0.9	0.9
Scalar/tensor lattice shift	−5.7	6.1	−0.3	0.9
Higher order lattice shifts	−0.2	0.3	−0.6	0.3
Probe light Stark shift	0	0.03	0	0.002
Cold collisions	1.6	4.1	0	0.1
Background gas collisions	−0.5	0.5	−0.2	0.2
2nd order Zeeman shift	10.9	0.5	3.3	0.1
Servo error	0	0.03	0	0.05
Tunneling	0	0	0	0.1
dc Stark shift	0	0.03	0	0.03
Total	494.4	7.4	495.6	2.6

vacuum chamber by Pt100 platinum resistance sensors with an expanded ($k = 2$) uncertainty of 40 mK [40], where we have taken care to cover the coolest and warmest spots. According to Ref. [57], we use $\overline{T} = (T_{\max} + T_{\min})/2$ as the representative temperature to calculate the BBR shift. We assign an uncertainty of $(T_{\max} - T_{\min})/\sqrt{12}$ as we assume the "true" temperature to lie with constant probability in the interval $[T_{\max}, T_{\min}]$. Typically, we observe $\Delta T \approx 0.4$ K resulting in an uncertainty contribution of about 9×10^{-18} [1,58]. The design of the coils and their precise temperature control are the main reasons for the highly homogeneous temperature.

Scalar and tensor lattice light shifts [59] are determined by monitoring the difference in frequency offsets between the TOC and the stationary clock when operating the former with thermally averaged lattice depths of 50.8 E_r and 88.8 E_r. Their uncertainty has been limited by the short measurement time available. The atomic temperature in the lattice of typically about 3.5 μK is derived from sideband spectra [60]. Higher-order light shifts are calculated using the coefficients given in Refs. [10,59].

The cold-collision shift is determined similarly by varying the atom number in the lattice. Background gas collision shifts are calculated based on the theory in Ref. [61], a lattice lifetime of 3 s, and coefficients from Ref. [62]. While the linear Zeeman shift is directly removed by the stabilization protocol, the quadratic Zeeman shift has to be corrected independently. This is straightforward as the line splitting provides a direct measure of the magnetic field sampled by the atoms as we operate the TOC at a configuration with vanishing vector light shift [59]. Tunneling between lattice sites is strongly suppressed due to the tilted and deep lattice [63]. The inner surfaces of the reentrant flanges, which are the surfaces closest to the atoms (Fig. 4), are coated with a conducting material (indium tin oxide) on top of an antireflective coating. With a separation of the windows of 54 mm, possible patch potentials of up to 100 mV, and the coefficient from [58], we estimate a maximum dc-Stark shift far below 1×10^{-18}. Other known uncertainties from servo errors, optical path length variations [64], and line pulling are below 10^{-18} and will not be discussed here.

During a first set of frequency ratio measurements, the 813 nm light for the optical lattice was generated by a diode laser and amplified by a tapered amplifier (TA) chip. Such laser systems are known to cause problems in the determination of the ac-Stark shift cancellation wavelength due to spectral impurities caused by amplified spontaneous emission [65]. Nevertheless, it had been chosen for its compactness and mechanical robustness. Despite additional efforts in spectral filtering and disentangling spatial and spectral impurities [40], the comparison of both Sr lattice clocks has revealed a fractional frequency difference of about 3×10^{-16} that is not compatible with the combined uncertainty of the clocks of below 1×10^{-16}.

After a reevaluation of the TOC with a Ti:sapphire laser as the lattice laser, we found $\nu_{\text{trans}}/\nu_{\text{stat}} - 1 = -6(80) \times 10^{-18}$ including a redshift correction of $-9.0(6) \times 10^{-18}$. The latter was determined by using a ruler, a spirit level, and the knowledge of the local gravity acceleration. Here we use the observed instability (Fig. 3) extrapolated to the full length of the data set of 1.5×10^{-17} as statistical uncertainty. The uncertainty budgets of both clocks are listed in Table I.

In conclusion, we have built and characterized a TOC that achieves a systematic uncertainty of 7.4×10^{-17} and an instability of $1.3 \times 10^{-15}/\sqrt{\tau}$. Note that the gross of the uncertainty stems from the uncertainty in the lattice light shift. This will be reduced significantly by a full characterization of the new lattice laser system. Therefore, we expect the BBR-related uncertainty to become the limiting uncertainty in the near future, which is already below 1×10^{-17} and can be reduced further by dedicated probes as presented in Ref. [39]. An interrogation laser with improved frequency stability is under development and will reduce the instability of the clock. Already now, our

TOC is outperforming the best transportable Cs fountain clock by 1 order of magnitude in systematic uncertainty and 2 orders in instability. Compared to the recently reported performance of the transportable Ca ion clock [31], our clock takes about 300-fold shorter averaging time to reach any given statistical uncertainty.

Already in the second off-campus campaign, we were able to perform spectroscopy of the reference transition within ten working days. BBR-related uncertainties where found to be similar to those reported here. In conclusion, our TOC is ready for applications like chronometric leveling, international clock comparisons, and precision measurements for fundamental physics.

This work was supported by QUEST, DFG through the RTG 1729 and CRC 1128 geo-Q, the Marie-Curie Action ITN FACT, and the EMRP project ITOC. The EMRP is jointly funded by the EMRP participating countries within EURAMET and the European Union.

[1] T. L. Nicholson *et al.*, Nat. Commun. **6**, 6896 (2015).
[2] N. Nemitz, T. Ohkubo, M. Takamoto, I. Ushijima, M. Das, N. Ohmae, and H. Katori, Nat. Photonics **10**, 258 (2016).
[3] N. Huntemann, C. Sanner, B. Lipphardt, C. Tamm, and E. Peik, Phys. Rev. Lett. **116**, 063001 (2016).
[4] M. Schioppo *et al.*, Nat. Photonics **11**, 48 (2017).
[5] A. Al-Masoudi, S. Dörscher, S. Häfner, U. Sterr, and C. Lisdat, Phys. Rev. A **92**, 063814 (2015).
[6] N. Hinkley, J. A. Sherman, N. B. Phillips, M. Schioppo, N. D. Lemke, K. Beloy, M. Pizzocaro, C. W. Oates, and A. D. Ludlow, Science **341**, 1215 (2013).
[7] Special issue on the measurement of time (La mesure du temps), F. Riehle, C.R. Phys. **16**, 506 (2015).
[8] H. Margolis, Nat. Phys. **10**, 82 (2014).
[9] C. Grebing, A. Al-Masoudi, S. Dörscher, S. Häfner, V. Gerginov, S. Weyers, B. Lipphardt, F. Riehle, U. Sterr, and C. Lisdat, Optica **3**, 563 (2016).
[10] R. Le Targat *et al.*, Nat. Commun. **4**, 2109 (2013).
[11] N. Huntemann, B. Lipphardt, C. Tamm, V. Gerginov, S. Weyers, and E. Peik, Phys. Rev. Lett. **113**, 210802 (2014).
[12] R. M. Godun, P. B. R. Nisbet-Jones, J. M. Jones, S. A. King, L. A. M. Johnson, H. S. Margolis, K. Szymaniec, S. N. Lea, K. Bongs, and P. Gill, Phys. Rev. Lett. **113**, 210801 (2014).
[13] T. M. Fortier *et al.*, Phys. Rev. Lett. **98**, 070801 (2007).
[14] M. Vermeer, *Chronometric Levelling*, Reports of the Finnish Geodetic Institute, Vol. No. 83:2 (Geodeettinen Laitos, Geodetiska Institutet, Helsinki, 1983), ISBN 9789517110877.
[15] A. Bjerhammar, Bulletin Géodésique **59**, 207 (1985).
[16] A. Bjerhammar, Technical Report NOS 118 NGS 36, NOAA (1986), http://www.ngs.noaa.gov/PUBS_LIB/RelativisticGeodesy_TR_NOS118_NGS36.pdf.
[17] C. Lisdat *et al.*, Nat. Commun. **7**, 12443 (2016).
[18] T. Takano, M. Takamoto, I. Ushijima, N. Ohmae, T. Akatsuka, A. Yamaguchi, Y. Kuroishi, H. Munekane, B. Miyahara, and H. Katori, Nat. Photonics **10**, 662 (2016).
[19] K. Predehl *et al.*, Science **336**, 441 (2012).
[20] S. M. F. Raupach, A. Koczwara, and G. Grosche, Phys. Rev. A **92**, 021801(R) (2015).
[21] N. Chiodo, N. Quintin, F. Stefani, F. Wiotte, E. Camisard, C. Chardonnet, G. Santarelli, A. Amy-Klein, P.-E. Pottie, and O. Lopez, Opt. Express **23**, 33927 (2015).
[22] D. Calonico *et al.*, Appl. Phys. B **117**, 979 (2014).
[23] P. Morzyński *et al.*, Sci. Rep. **5**, 17495 (2015).
[24] H. Hachisu *et al.*, Opt. Lett. **39**, 4072 (2014).
[25] M. Niering *et al.*, Phys. Rev. Lett. **84**, 5496 (2000).
[26] M. Fischer *et al.*, Phys. Rev. Lett. **92**, 230802 (2004).
[27] C. G. Parthey *et al.*, Phys. Rev. Lett. **107**, 203001 (2011).
[28] Special issue on the measurement of time (La mesure du temps), K. Bongs *et al.*, C.R. Phys. **16**, 553 (2015).
[29] N. Poli, M. Schioppo, S. Vogt, S. Falke, U. Sterr, C. Lisdat, and G. M. Tino, Appl. Phys. B **117**, 1107 (2014).
[30] G. Mura, T. Franzen, C. A. Jaoudeh, A. Görlitz, H. Luckmann, I. Ernsting, A. Nevsky, S. Schiller, and the SOC2 Team, in *Proc. IFCS-EFTF 2013* (2013).
[31] J. Cao, P. Zhang, J. Shang, K. Cui, J. Yuan, S. Chao, S. Wang, H. Shu, and X. Huang, arXiv:1607.03731.
[32] J. Lodewyck *et al.*, Metrologia **53**, 1123 (2016).
[33] S. Falke *et al.*, New J. Phys. **16**, 073023 (2014).
[34] S. Bize *et al.*, C.R. Phys. **5**, 829 (2004).
[35] M. Abgrall, Frequency Comparison (H_MASER 140 0889)-(LNE-SYRTE-FOM) for the period MJD 56154 to MJD 56169 (2012), http://www.bipm.org/en/bipm-services/timescales/time-ftp/data.html.
[36] J. Guéna *et al.*, IEEE Trans. Ultrason. Ferroelectr. Freq. Control **59**, 391 (2012).
[37] S. Vogt, Ph.D. thesis, QUEST-Leibniz-Forschungsschule der Universität Hannover, 2015, http://edok01.tib.uni-hannover.de/edoks/e01dh15/837746116.pdf.
[38] S. Vogt, S. Häfner, J. Grotti, S. Koller, A. Al-Masoudi, U. Sterr, and C. Lisdat, J. Phys. Conf. Ser. **723**, 012020 (2016).
[39] B. J. Bloom, T. L. Nicholson, J. R. Williams, S. L. Campbell, M. Bishof, X. Zhang, W. Zhang, S. L. Bromley, and J. Ye, Nature (London) **506**, 71 (2014).
[40] See Supplemental Material at http://link.aps.org/supplemental/10.1103/PhysRevLett.118.073601 for details, which includes Refs. [59,41–43].
[41] H. Preston-Thomas, Metrologia **27**, 3 (1990), see erratum Ref. [42], for T-T90 also see Ref. [43].
[42] H. Preston-Thomas, Metrologia **27**, 107 (1990).
[43] J. Fischer, M. de Podesta, K. D. Hill, M. Moldover, L. Pitre, R. Rusby, P. Steur, O. Tamura, R. White, and L. Wolber, Int. J. Thermophys. **32**, 12 (2011).
[44] S. Häfner, S. Falke, C. Grebing, S. Vogt, T. Legero, M. Merimaa, C. Lisdat, and U. Sterr, Opt. Lett. **40**, 2112 (2015).
[45] S. Häfner, Ph.D. thesis, Leibniz Universität Hannover, 2015, http://edok01.tib.uni-hannover.de/edoks/e01dh16/84568972X.pdf.
[46] U. Sterr, Frequenzstabilisierungsvorrichtung German Patent No. DE 10 2011 015 489 (2011), https://depatisnet.dpma.de/DepatisNet/depatisnet?action=bibdat&docid=DE102011015489B3.
[47] S. Vogt, C. Lisdat, T. Legero, U. Sterr, I. Ernsting, A. Nevsky, and S. Schiller, Appl. Phys. B **104**, 741 (2011).
[48] H. Katori, in *Proceedings of the Sixth Symposium on Frequency Standards and Metrology, 9–14 September 2001, St. Andrews, Scotland*, edited by P. Gill (World Scientific, Singapore, 2002), pp. 323–330.

[49] S. Falke *et al.*, Metrologia **48**, 399 (2011).

[50] G. J. Dick, in *Proceedings of 19th Annu. Precise Time and Time Interval Meeting, Redendo Beach, 1987* (U.S. Naval Observatory, Washington, DC, 1988), pp. 133–147, http://tycho.usno.navy.mil/ptti/1987papers/Vol%2019_13.pdf.

[51] C. W. Chou, D. B. Hume, J. C. J. Koelemeij, D. J. Wineland, and T. Rosenband, Phys. Rev. Lett. **104**, 070802 (2010).

[52] Y.-G. Lin, Q. Wang, Y. Li, F. Meng, B.-K. Lin, E.-J. Zang, Z. Sun, F. Fang, T.-C. Li, and Z.-J. Fang, Chin. Phys. Lett. **32**, 090601 (2015).

[53] S. Lee, C. Y. Park, W.-K. Lee, and D.-H. Yu, New J. Phys. **18**, 033030 (2016).

[54] H. Hachisu and T. Ido, Jpn. J. Appl. Phys. **54**, 112401 (2015).

[55] I. R. Hill, R. Hobson, W. Bowden, E. M. Bridge, S. Donnellan, E. A. Curtis, and P. Gill, J. Phys. Conf. Ser. **723**, 012019 (2016).

[56] R. Tyumenev *et al.*, New J. Phys. **18**, 113002 (2016).

[57] GUM, Guide to the Expression of Uncertainty in Measurement, ISO/TAG 4. (ISO, 1993) (corrected and reprinted, 1995) in the name of the BIPM, IEC, IFCC, ISO, UPAC, IUPAP, and OIML (Sèrres, France, 1995), ISBN 92-67-10188-9, 1995.

[58] T. Middelmann, S. Falke, C. Lisdat, and U. Sterr, New J. Phys. **14**, 073020 (2012).

[59] P. G. Westergaard, J. Lodewyck, L. Lorini, A. Lecallier, E. A. Burt, M. Zawada, J. Millo, and P. Lemonde, Phys. Rev. Lett. **106**, 210801 (2011).

[60] S. Blatt, J. W. Thomsen, G. K. Campbell, A. D. Ludlow, M. D. Swallows, M. J. Martin, M. M. Boyd, and J. Ye, Phys. Rev. A **80**, 052703 (2009).

[61] K. Gibble, Phys. Rev. Lett. **110**, 180802 (2013).

[62] J. Mitroy and J. Y. Zhang, Mol. Phys. **108**, 1999 (2010).

[63] P. Lemonde and P. Wolf, Phys. Rev. A **72**, 033409 (2005).

[64] S. Falke, M. Misera, U. Sterr, and C. Lisdat, Appl. Phys. B **107**, 301 (2012).

[65] R. Le Targat, L. Lorini, M. Gurov, M. Zawada, R. Gartman, B. Nagorny, P. Lemonde, and J. Lodewyck, in *European Frequency and Time Forum (EFTF), 2012* (IEEE, Gothenburg, 2012), contribution to European Frequency and Time Forum 2012, Gothenburg, Sweden.